Comparison of Chromatic Dispersion of Circular and Hexagonal Photonic Crystal Fibers with Chloroform-Core

Tran Tran Bao Le[1*], Oanh Truong Thi Chuyen[2], Thuy Nguyen Thi[3], Lanh Chu Van[1]
1- Department of Physics, Vinh University, Vinh, Vietnam.
Email: letranbaotran212@gmail.com (Corresponding author), chuvanlanh@vinhuni.edu.vn
2- Nguyen Quang Dieu High School for the Gifted, Cao Lanh, Vietnam.
Email: ttcoanhkv@gmail.com
3- University of Education, Hue University, Hue, Vietnam.
Email: ntthuy@hueuni.edu.vn

Received: May 2022 Revised: May 2022 Accepted: June 2022

ABSTRACT:
In this paper, we compare dispersion characteristics of chloroform-core photonic crystal fibers (PCFs) with circular lattice and hexagonal lattice in the case of different air hole diameters. By varying lattice constant Λ and filling factor in the first ring d_1/Λ, we can easily control chromatic dispersion and achieve three optimal structures for the circular lattice of fibers #CF_1 (Λ = 1.0 µm, d_1/Λ = 0.65), #CF_2 (Λ = 1.0 µm, d_1/Λ = 0.7), and #CF_3 (Λ = 2.0 µm, d_1/Λ = 0.3) and two optimal structures for the hexagonal lattice of fibers #HF_1 (Λ = 1.0 µm, d_1/Λ = 0.5), #HF_2 (Λ = 2.0 µm, d_1/Λ = 0.3). At the same structural parameter (Λ = 2.0 µm, d_1/Λ = 0.3) and the corresponding pumping wavelength, the circular structure has a dispersion smaller by 5.598 ps/mn/km than the hexagonal lattice. #CF_1 has all-normal dispersion with the peak of the dispersion curve asymptote to the zero-dispersion curve which is very suitable for coherent supercontinuum generation (SCG). The #HF_1 structure has a near-zero flat anomalous dispersion in the wide wavelength range from 1.1 µm to 1.4 µm. Our results will be an important premise in choosing a PCF structure to study SCG.

KEYWORDS: Photonic Crystal Fibers, Chloroform, Dispersion Characteristic, Circular Lattice, Hexagonal Lattice.

1. INTRODUCTION

The appearance of Photonic Crystal Fibers (PCFs) is great progress in the field of optical communication. Unlike conventional optical fibers, PCF is a special type of optical fiber with a structure of many air holes running along its axis with a core in the center of the fiber [1]. PCF includes solid-core fiber and hollow-core fiber with completely different light transmission mechanisms. A solid-core PCF transmits the light based on total internal reflection. The discovery of solid-core PCF has been widely applied in science and technology, especially in the field of fiber-optic communication because of its outstanding advantages such as low loss, high nonlinearity, and wider dispersion range compared to conventional optical fiber… However, solid-core PCF also has certain limitations in terms of flat dispersion, leading to drawbacks in the study of supercontinuum generation (SCG) [2]. On the other hand, hollow-core PCFs have a photonic bandgap light-guiding mechanism. In which, the refractive index of the core is smaller than that of the lattice cladding; the cyclically arranged air holes may be hollow or contain material such as a liquid or a gas. The light entering the PCFs is confined in the hollow core by the barrier of the photonic bandgap made up of cyclic air holes arrays surrounding the core.

From many research results, it is shown that there is a great influence of the structural parameters of PCF on the characteristics such as dispersion, loss, effective mode area... Among them, the control of dispersion characteristics brings positive results and opens up a wide range of interesting research for scientists. A photonic feed system for a four-arm sinuous antenna was designed using a hybrid approach based on the difference between dispersive and non-dispersive delay [3]. Hossein et al. [4] practically demonstrated a microwave photonic frequency measurement receiver employing four-wave mixing in an optical fiber with high nonlinearity and its ability to become dynamically reconfigured through wavelength tuning in a dispersive fiber. Sensitivity could be improved by Lock-In techniques, making for a very attractive microwave photonic instantaneous frequency measurement system [5]. Especially, chromatic dispersion plays an important

Paper type: Research paper
DOI: https://doi.org/10.52547/mjee.16.3.55
How to cite this paper: T. Tran Bao Le, O. Truong Thi Chuyen, Th. Nguyen Thi, L. Chu Van, **"Comparison of Chromatic Dispersion of Circular and Hexagonal Photonic Crystal Fibers with Chloroform-Core"**, Majlesi Journal of Electrical Engineering, Vol. 16, No. 3, pp. 55-61, 2022.

role in looking for the optimal PCFs for SCG applications. To facilitate the adjustment of the dispersion curve, selective liquids can be infiltrated into the core of the PCF [6-9]. With different nonlinear indices of liquids, we can control the dispersion characteristic of PCF without changing the geometric structure of the fiber [6-9]. Optimized PCFs are widely used in many fields from telecommunications to metrology, spectroscopy, microscopy, medical diagnostics, biology, and sensing.

Besides, the geometrical structure in the cladding of the fiber also has a significant influence on the characteristics of PCF. Up to now, there have been much research works on filling liquid into PCFs with circular lattice, hexagonal lattice, and square lattice,… and have obtained positive results, especially the application of optimal PCF fibers in the supercontinuum development [7-10]. Among them, the circular and hexagonal lattices have received a lot of attention from researchers because of their ability to enhance the nonlinearity of the fibers, especially the flat and low dispersion curves for hexagonal lattices, and effective mode area minimization for circular lattices. This has been confirmed by several published studies [10-13]. However, most of these studies have only focused on optimizing the chromatic dispersion of each geometry, but have not evaluated yet which lattice has more optimal dispersion for the SCG. To clarify this issue, we carried out liquid infiltration of $CHCl_3$ into the hollow-core of PCF with circular and hexagonal lattices to compare their dispersion characteristics with each other. With high nonlinearity, $CHCl_3$ is a good candidate for enhancing the efficiency of SCG.

The PCFs that we analyzed are novel structures with eight air hole rings arranged in a circular or a hexagonal lattice with a hollow core filled with $CHCl_3$. In which, we change the air hole diameter of the first ring which is represented by the change in filling factor d_1/Λ and the lattice constant Λ and numerically simulate dispersion characteristics using Lumerical Mode Solution software. This is a new point in the study of PCF structures compared with previous publications with the air hole diameter in the rings being constant [7-9], [12-15].

2. STRUCTURAL DESCRIPTION AND THEORY OF DISPERSION IN THE PCF

To increase the linearity of PCFs, it is common to infiltrate liquid into the core of the fiber to optimize its characteristics. Liquids commonly used are carbon disulfide (CS_2), and carbon tetrachloride (CCl_4) [13-16] In publication [17], the nonlinear refractive index of CS_2 is by a factor of approximately 200 times higher than that of silica (SiO_2), supercontinuum in the near-infrared (NIR), and mid-infrared (MIR) regions can be generated in the CS_2-filled fibers. However, as shown in Fig. 1, the material dispersion of CS_2 is much larger than that of SiO_2. It is for this reason that the generation of supercontinuum from the visible to NIR region of CS_2-PCFs is limited because it is difficult to compensate for the high material dispersion in the visible region.

From Fig. 1, it is shown that compared with CS_2, material dispersions and the refractive indices in CCl_4 and $CHCl_3$ are closer to those in SiO_2. Moreover, the material dispersion in $CHCl_3$ is lower than that of CCl_4 in the visible light region and the nonlinear refractive index of $CHCl_3$ is greater than that of CCl_4. For this reason, PCF with a core filled with $CHCl_3$ is selected for the study.

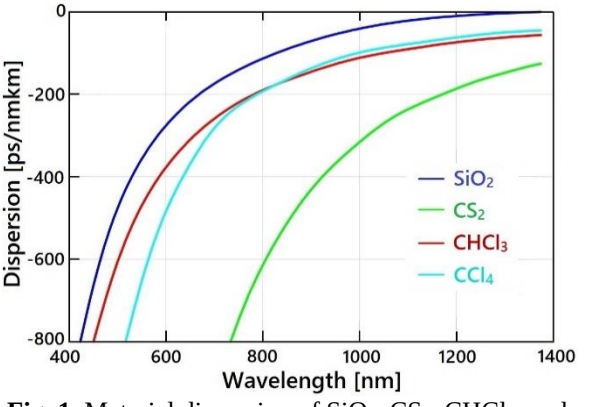

Fig. 1. Material dispersion of SiO_2, CS_2, $CHCl_3$, and CCl_4 [17].

The chromatic dispersion of PCF is calculated according to [5]

$$D = -\frac{\lambda}{c}\frac{d^2\,\mathrm{Re}(n_{eff})}{d\lambda^2} \tag{1}$$

Where c is the speed of light in a vacuum, $\mathrm{Re}(n_{eff})$ is the real part of the effective refractive index, and λ is the wavelength which has the dimension of micrometer (μm).

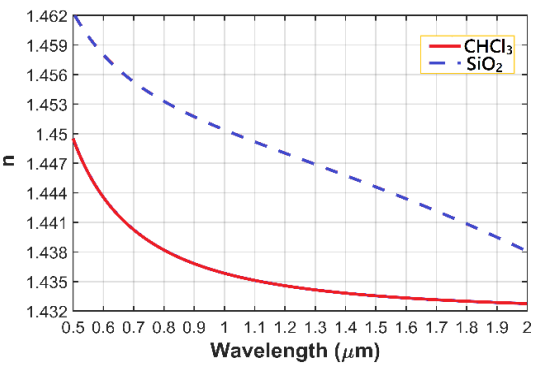

Fig. 2. A real part of the refractive index of $CHCl_3$ and SiO_2.

$CHCl_3$ has a high nonlinear refractive index of 29.6×10^{-20} m^2/W [18] which is nearly 11 times larger

than that of SiO_2 with a refractive index of 2.74×10^{-20} m^2/W at 1053 nm [19]. This nonlinearity allows the PCF to generate a much wider spectrum with low input power; in short propagation distance, high nonlinearity is important for the enhancement of SCG efficiency. Fig. 2 shows the difference between the real fraction of the refractive index of $CHCl_3$ and SiO_2.

Linear refractive index n of $CHCl_3$ as a function of wavelength is described by Sellmeier's formula [8]

$$n(\lambda)=\sqrt{1+\frac{A_1\lambda^2}{\lambda^2-B_1}+\frac{A_2\lambda^2}{\lambda^2-B_2}+\frac{A_3\lambda^2}{\lambda^2-B_3}} \quad (2)$$

Where the corresponding parameters B_1, B_2, B_3 and C_1, C_2, C_3 are listed in Table 1.

Table 1. Dispersion parameters of SiO_2 and $CHCl_3$.

Coefficient	Material	
	SiO_2	$CHCl_3$
A_1	0.6694226	1.04647
B_1 (μm^2)	4.4801×10^{-3}	0.01048
A_2	0.4345839	0.00345
B_2 (μm^2)	1.3285×10^{-2}	0.15207
A_3	0.8716947	
B_3 (μm^2)	95.341482	

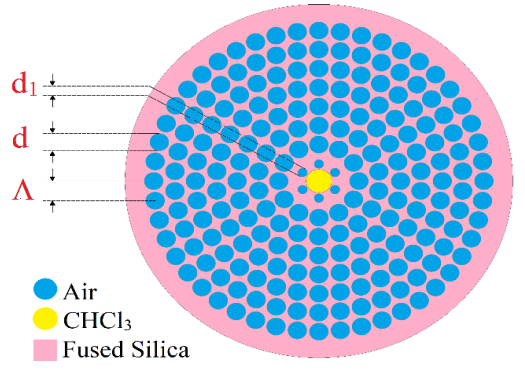

a)

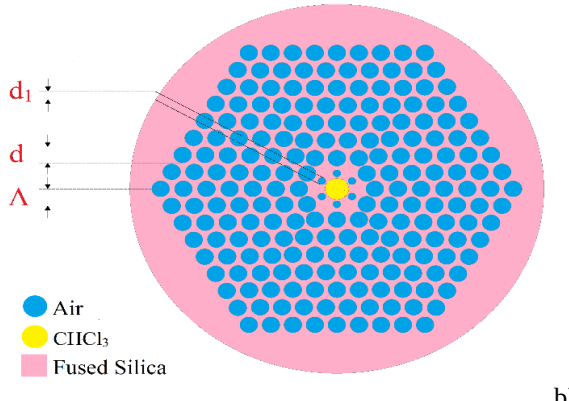

b)

Fig. 57. The geometrical structure of PCF with the circular lattice (a) and hexagonal lattice (b).

In this paper, we compare the dispersion of two $CHCl_3$-core PCFs with circular and hexagonal lattices with SiO_2 as the substrate material. The cross-section of the PCF structure is shown in Fig. 3.

Both structures have eight air hole rings with lattice constant Λ, the first ring has a diameter of d_1, and the remaining rings have a diameter of d. The large core is filled with $CHCl_3$ with a diameter $D_c = 2\Lambda - 1.1d_1$, where the value of lattice constant is as follows: Λ = 1.0 µm, 1.5 µm, 2.0 µm, 2.5 µm. The increase in the filling factor d_1/Λ from 0.3 to 0.8 helps change the diameter of the first ring differently from the rest, a difference compared to many previous publications with the same diameters of the air holes in all rings [7-9], [12-15]. Thus, the circular and hexagonal PCFs in our work are new structures with flexibility in dispersion management that will well support the search for optimal fibers for SCG application.

3. RESULTS AND DISCUSSION

Figs. 4 and 5 show the dispersion characteristic of $CHCl_3$-filled PCFs with circular and hexagonal lattices. It can be seen that most of the structures have one or two zero-dispersion wavelengths (ZDW). When the filling factor d_1/Λ gradually increases from 0.3 to 0.8, i.e the core diameter D_c reduces, the slope of the dispersion curve also increases in the wavelength range from 0.7 µm to 0.9 µm.

Fig. 4 shows that the circular lattice structure possesses all-normal dispersion with fibers with d_1/Λ = 0.5–0.65 at Λ = 1.0 µm, where the dispersion curve of PCF corresponding to d_1/Λ = 0.65 is the closest to the zero-dispersion curve. The remaining cases of the lattice constant appear anomalous dispersion intersecting the zero-dispersion line at one or two points.

For the hexagonal PCF, in all cases, there is no all-normal dispersion, only anomalous dispersion curves in the whole investigated wavelength range (Fig. 5).

From the observation of the figures, we can see that the dispersion curves of most structures are extended toward longer wavelengths with increasing filling factors, and ZDWs are obtained in the NIR region. As is known, chromatic dispersion is one of the factors that strongly affect the efficiency of SCG; the flatter the dispersion and the closer it is to zero dispersion, the larger the supercontinuum bandwidth is. In the next step, we select the optimal structures with near-zero flat dispersion curves for each type of lattice.

For circular lattice PCFs, we choose three optimal structures including:

- #CF_1: Λ = 1.0 µm, d_1/Λ = 0.65, D_c = 1.285 µm
- #CF_2: Λ = 1.0 µm, d_1/Λ = 0.7, D_c = 1.23 µm
- #CF_3: Λ = 2.0 µm, d_1/Λ = 0.3, D_c = 3.34 µm

The dispersion characteristics of these structures are illustrated in Fig. 4.

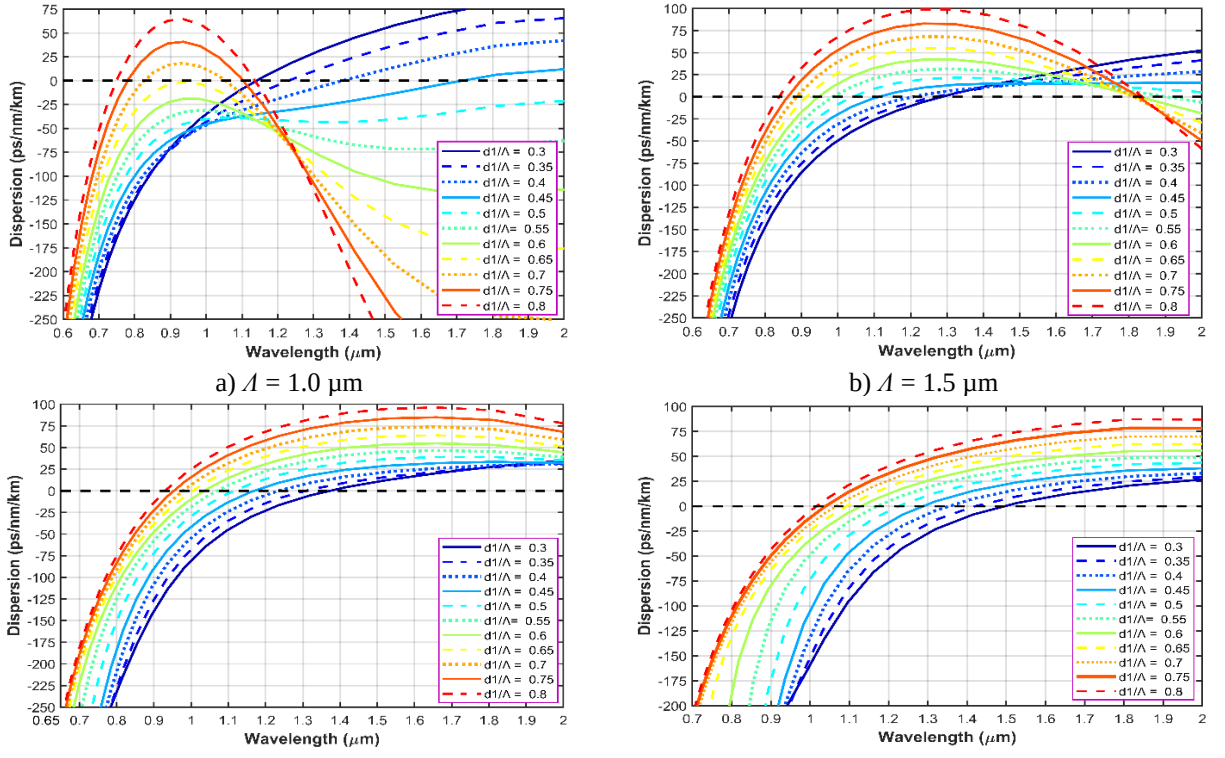

a) Λ = 1.0 µm b) Λ = 1.5 µm

c) Λ = 2.0 µm d) Λ = 2.5 µm

Fig. 4. Graph of the dispersion characteristic *D* of the circular lattice structure filled by $CHCl_3$.

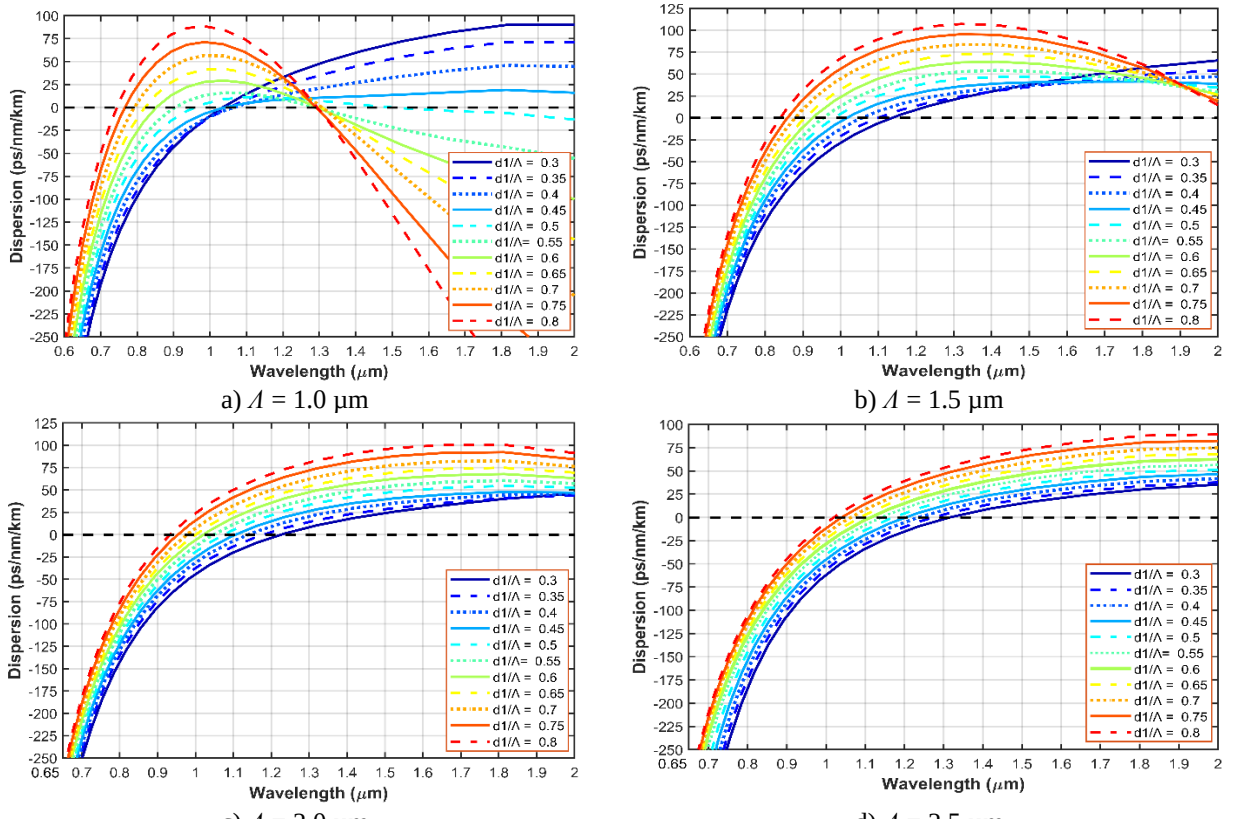

a) Λ = 1.0 µm b) Λ = 1.5 µm

c) Λ = 2.0 µm d) Λ = 2.5 µm

Fig. 5. Graph of the dispersion characteristic *D* of the hexagonal lattice structure filled by $CHCl_3$.

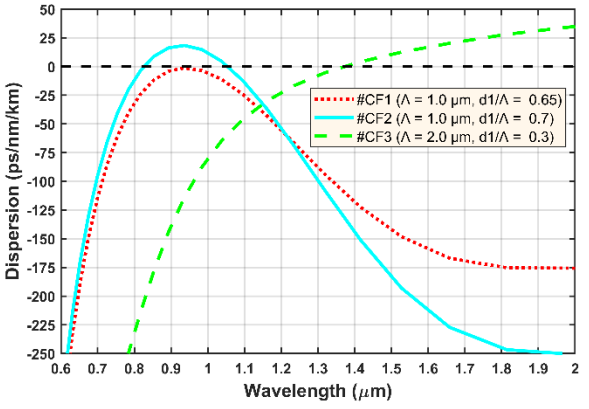

Fig. 6. The optimal dispersion structures of the circular lattice.

From Fig. 6, we can see that #CF_1 (red curve) appears all-normal dispersion which is asymptotic to the zero-dispersion line, while the #CF_2 fiber exits two ZDWs at 0.827 μm and 1.053 μm; the #CF_3 fiber has a ZDW at 1.374 μm.

For the hexagonal lattice, we obtain two optimal structures:

- #HF_1: Λ = 1.0 μm, d_1/Λ = 0.5, D_c = 1.45 μm
- #HF_2: Λ = 2.0 μm, d_1/Λ = 0.3, D_c = 3.34 μm

Fig. 7 illustrates the dispersion characteristic of the proposed PCFs for the hexagonal lattice. As is observed, both structures exhibit anomalous dispersion. The #HF_1 fiber has ZDW_1 at 0.96 μm, its dispersion curve then moves to the negative side and crosses the zero-dispersion line at ZDW_2 = 1.501 μm. Meanwhile, #HF_2 has a ZDW at 1.227 μm.

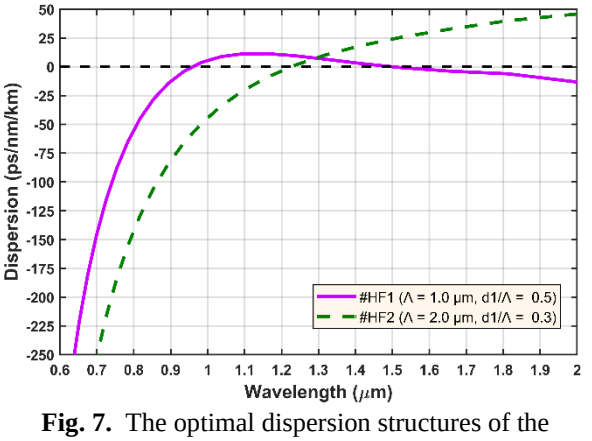

Fig. 7. The optimal dispersion structures of the hexagonal lattice.

To facilitate the comparison of the dispersion characteristics of the two lattices, we synthesize the dispersion curves of the optimal structures as shown in Fig. 8.

From Fig. 8, we notice that the #CF_2 and #HF_1 structures both have anomalous dispersion curves and intersect the zero-dispersion line at two points. However, the peak of the dispersion curve of #HF_1 is close to the zero-dispersion line than #CF_2, and its flatness is maintained in the wavelength range from 1.1 μm to 1.4 μm in the anomalous dispersion regime. With the above properties, we select the pump wavelength (λ_p) for #CF_2 and #HF_1 to be 0.945 μm and 1.3 μm, respectively. Meanwhile, the #CF_1 fiber has near-zero all-normal dispersion and a wavelength at the maximum dispersion very close to the pump wavelength of 0.945 μm, which is very favorable for SCG with high coherence. Structures #CF_3 and #HF_2 have anomalous dispersion with one ZDW. In which, the #CF_3 fiber has a lower dispersion curve and is close to the zero-dispersion line than that of #HF_2, and is expected to be pumped at 1.4 μm while #HF_2 has a pump wavelength of 1.3 μm. The dispersion values of the structures at the pump wavelength are given in Table 2.

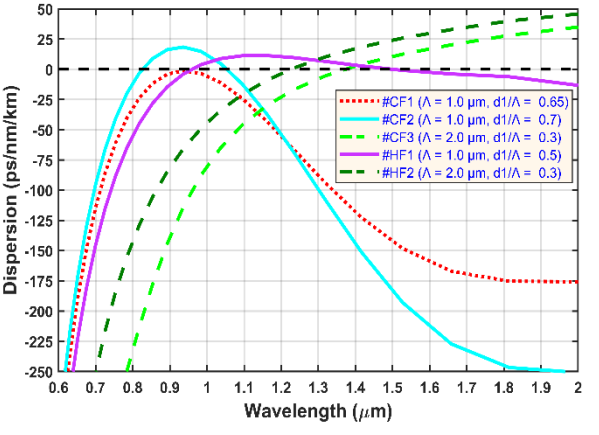

Fig. 8. The optimal dispersion structures of the hexagonal lattice.

Table 2. The dispersion values of the optimal structures for the two lattices at the pump wavelength.

#	ZDW (μm)	λ_p (μm)	D (ps/nm/km)
#CF_1	-	0.945	-1.623
#CF_2	ZDW_1 = 0.827 ZDW_2 = 1.053	0.945	17.726
#CF_3	1.374	1.4	2.612
#HF_1	ZDW_1 = 0.96 ZDW_2 = 1.501	1.3	7.234
#HF_2	1.227	1.3	8.21

The results in Table 2 show that the #CF_3 fiber has a dispersion of 2.612 ps/nm/km at 1.4 μm which is smaller than that of #HF_2 (8.21 ps/nm/km at 1.3 μm) at the same core diameter. At the pump wavelength of 0.945 μm, the dispersion value of #CF_1 is quite low, equal to -1.623 ps/nm/km. In general, the circular lattice structure has the advantage of small dispersion, while the hexagonal lattice provides flat dispersion in a wide wavelength region demonstrated by the #HF_1 fiber. In all cases, the dispersion value of #CF_2 fiber at 0.945 μm pumping

wavelength is the largest, with 17.726 ps/nm/km, approximately 2.5 times larger than that of the #HF_1 structure (7.234 ps/nm/km at 1.3 μm). However, this number is still smaller than some previous works [9], [15]. In the case of all-normal dispersion, the dispersion of #CF_1 is much smaller than that of publications with the uniform model of air holes [8], [15]; it is even smaller than that of publications considering the change in the air hole diameter of the rings as ours [12]. These results are shown in Table 3, confirming the superiority of our model in optimizing the dispersion characteristics for SCG.

Table 3. The optical properties of the selected PCFs and those previously published.

Optimal fibers	Regime	Λ (μm)	d_1/Λ	D_c (μm)	λ_p (μm)	D (ps/nm/km)
[8]	All-normal	1.0	0.65	1.285	1.03	-24
[9]	Anomalous	1.0	0.8	1.12	1.03	33.7
[9]	Anomalous	1.5	0.8	1.68	1.56	110
[15]	All-normal	1.5	0.65	2.28	1.03	-38.8
[15]	Anomalous	1.5	0.4	1.83	1.03	18.5
[11]	All-normal	1.0	0.65	1.285	1.15	-31.8
#CF_1	All-normal	1.0	0.65	1.285	0.945	-1.623
#CF_2	Anomalous	1.0	0.7	1.23	0.945	17.726
#CF_3	Anomalous	2.0	0.3	3.34	1.4	2.612
#HF_1	Anomalous	1.0	0.5	1.45	1.3	7.234
#HF_2	Anomalous	2.0	0.3	3.34	1.3	8.21

4. CONCLUSION

In this paper, we compare the dispersion characteristics of PCF with the circular lattice and hexagonal lattice when their core is filled with $CHCl_3$. By varying the lattice constant Λ and the filling factor d_1/Λ to vary the air hole diameter of the first ring, we can flexibly control dispersion characteristics and obtain the optimal structures of the two lattices. At the same parameter Λ = 2.0 μm, d_1/Λ = 0.3, and D_c = 3.34 μm, the circular lattice structure (#CF_3) has more optimal dispersion than hexagonal lattice (#HF_2) because its dispersion at 1.3 μm pump wavelength less than 5.598 ps/nm/km. The #CF_1 fiber possesses all-normal dispersion and has a maximum point of the dispersion curve that is asymptotic to the zero-dispersion line; the wavelength corresponding to this point has very little difference from the pump wavelength. This is a favorable condition of the structure with a circular lattice for highly coherent SCG that the hexagonal PCF does not have. Besides, the #HF_1 structure has a flatter anomalous dispersion curve than #CF_2, especially in the wavelength range from 1.1 μm to 1.4 μm, which is also a good candidate for SCG with a smooth spectrum in a wide wavelength range. This result again shows the superiority of varying the air hole diameter of the first ring in our new structure resulting in a flatter dispersion and smaller than that of the homogeneous fiber PCFs. The nonlinear refractive index of the infiltrated liquid into the fiber core also significantly affects the dispersion characteristic of PCF. In addition, we obtain the ZDW of the optimal structures in the NIR region, making favorable conditions for the selection of fiber structures for application in near-infrared SCG.

5. ACKNOWLEDGMENT

This research was funded by Vingroup JSC and supported by the Master, PhD Scholarship Programme of Vingroup Innovation Foundation (VINIF), Institute of Big Data, code [VINIF.2021.TS.155].

REFERENCES

[1] J. C. Knight, T. A. Birks, P. St. J. Russell, and D. M. Atkin, **"All-silica single-mode optical fiber with photonic crystal cladding, "** *Opt. Lett.*, Vol. 21, pp. 1547-1549, Oct. 1996.

[2] R. Buczyński, **"Photonic crystal fibers, "** *Acta Phys. Pol. Series A*, Vol. 106, pp. 141-168, Aug. 2004.

[3] E. Hossein, S. Niusha, R. L. L. Elias, and M. Arnan, **"Reconfigurable Photonic Feed for Sinuous Antenna,"** *J. Lightwave Tec.*, Vol. 30, pp. 2725-2732, Aug. 2012.

[4] E. Hossein, A. Mohsen, and E. H. Majid, **"Dynamically Reconfigurable All Optical Frequency Measurement System,"** *J. Lightwave Tec.*, Vol. 32, pp. 4194-4200, Dec. 2014.

[5] S. Niusha, E. Hossein, B. Lam, and M. Arnan, **"Microwave photonic instantaneous frequency measurement with improved sensitivity,"** presented at *2009 IEEE MTT-S Int. Microwave Symposium Digest*, Boston, USA, 2009.

[6] V. T. M. Ngoc, L. T. B. Tran, D. V. Trong, L. X. Bao, T. N. Thao, V. D. Long, T. V. Thanh, T. T. C. Oanh, H. T. A. Thu, N. T. Thuy, T. Q. Vu, and C. V. Lanh, **"Optimal structure of photonic crystal fiber with infiltrated benzen core for application supercontinuum generation,"** *in Proc. the 7th Academic Conf. on Natural Science for Young Scientists, Master and PhD. Students from Asean Countries*, pp. 397-405, 2021.

[7] P. Kumar and A. Mishra, **"PCF structure with circular air hole and square lattice and its high**

birefringence and lower zero dispersion behavior, " *Int. J. Electronics Communication and Computer Engineering*, Vol. 4, pp. 192-195, Jan. 2013.

[8] C. V. Lanh, H. V. Thuy Hoang, C. L. Van, K. Borzycki, D. X. Khoa, T. Q. Vu, M. Trippenbach, R. Buczyński, and J. Pniewski, **"Optimization of optical properties of photonic crystal fibers infiltrated with chloroform for supercontinuum generation, "** *Las. Phys.*, Vol. 29, 075107 (9pp), May 2019.

[9] C. V. Lanh, H. V. Thuy Hoang, C. L. Van, K. Borzycki, D. X. Khoa, T. Q. Vu, M. Trippenbach, R. Buczyński, and J. Pniewski, **"Optimization of optical properties of photonic crystal fibers infiltrated with chloroform for supercontinuum generation, "** *Las. Phys.*, Vol. 30, 035105 (9pp), Feb. 2020.

[10] N. T. Thuy, H. T. Duc, L. T. B. Tran, D. V. Trong, and C. V. Lanh, **"Optimization of optical properties of toluene-core photonic crystal fibers with circle lattice for supercontinuum generation, "** *J. Opt.*, Jan. 2022.

[11] C. V. Lanh, N. T. Thuy, H. T. Duc, L. T. B. Tran, V. T. M. Ngoc, D. V. Trong, L. C. Trung, H. D. Quang, and D. Q. Khoa, **"Comparison of supercontinuum spectrum generating by hollow core PCFs filled with nitrobenzene with different lattice types, "** *Opt. Quant. Electron.*, Vol. 54, 300 (17pp), Apr. 2022.

[12] C. V. Lanh, A. Anuszkiewicz, A. Ramaniuk, R. Kasztelanic, D. X. Khoa, C. L. Van, M. Trippenbach, and R. Buczyński, **"Supercontinuum generation in photonic crystal fibres with core filled with toluene, "** *J. Opt.*, Vol. 19, 125604 (9pp), Nov. 2017.

[13] D. T. Linh, P. N. Huyen, N. Q. Vu, N. L. Huong, T. Q. Vu, D. X. Khoa, and C. V. Lanh, **"Optimization of characteristic parameters of photonic crystal fiber with core infiltrated by carbon disulfide liquid for supercontinuum generation,"** *in Proc. the 5th Conf. on Advances in Appl. Engineering Phys. – CAEP V*, pp. 206-211, 2018.

[14] Mu'iz Maidi, Pg E. Abas, Pg I. Petra, S. Kaijage, N. Zou, and F. Begum, **"Theoretical considerations of photonic crystal fiber with all uniform-sized air holes for liquid sensing, "** *Photonics*, Vol. 8, 249 (14pp), Jun. 2021.

[15] L. V. Hieu, H. V. Thuy, L. C. Trung, H. D. Quang, N. T. Hue, V. T. M. Ngoc, M. Klimczak, R. Buczyński, and R. Kasztelanic, **"Silica-based photonic crystal fiber infiltrated with 1,2-dibromoethane for supercontinuum generation, "** *Appl. Opt.*, Vol. 60, pp. 7268-7278, Aug. 2021.

[16] D. T. Nhat, N. M. Linh, D. L. Chi, N. T. Trang, T. Q. Vu, D. X. Khoa, and C. V. Lanh, **"Photonic crystal fiber with core infiltrated by carbon tetrachloride for nonlinear effects generation,"** *in Proc. the 5th Conf. on Advances in Appl. Engineering Phys. – CAEP V*, pp. 200-205, 2018.

[17] C. Wanga, W. Lia, N. Lia, and W. Wang, **"Numerical simulation of coherent visible-to-near-infrared supercontinuum generation in the $CHCl_3$-filled photonic crystal fiber with 1.06 μm pump pulses, "** *Opt. Las. Tec.*, Vol. 88, pp. 215-221, Feb. 2017.

[18] P. P. Ho and R. R. Alfano, **"Optical Kerr effect in liquids, "** *Phys. Rev. A*, Vol. 20, pp. 2170-2187, Nov. 1979.

[19] S. Kedenburg, A. Steinmann, R. Hegenbarth, T. Steinle, and H. Giessen, **"Nonlinear refractive indices of nonlinear liquids: wavelength dependence and influence of retarded response, "** *Appl. Phys. B*, Vol. 117, pp. 803-816, Apr. 2014.